Muhammad USMAN

Department of Electrical Engineering, College of Engineering, University of Hail, Kingdom of Saudi Arabia

doi:10.15199/48.2016.06.31

Design Estimations and Channel Capacity Calculations for Spatial, Polarized MIMO Antenna System for Mobile Applications

Abstract. *Mobile MIMO (Multiple Input Multiple Output) communications provides an improved transmission capacity and error performance over traditional digital transmission systems. In this paper the spatial, polarization technique is used in order to improve the channel capacity of the proposed system. The potential for integrating MIMO systems comprising both 2×2 and 3×3 elements into a mobile handset environment will be considered. The MIMO channels will be subject to Rayleigh fading, and the results are compared against linear (or planar) arrays. In addition, different azimuthal spectra will be considered in evaluating the actual system performance.*

Streszczenie. *W artykule opisano wykorzystanie techniki przestrzennej polaryzacji anteny w celu poprawy pojemności systemu przesyłowego MIMO. System składa się z dwóch 2x2 i 3x3 elementów przystosowanych do odbiorników przenośnych.* ***Projektowanie i obliczanie pojemności kanałów w przestrzennym spolaryzowanym systemie anten MIMO w zastosowaniu do urządzeń przenośnych***

Keywords: MIMO, Channel Capacity, Polarization, Rayleigh Fading Channel.
Słowa kluczowe: system MIMO, antena, polaryzacja, pojemność kanału

Introduction

Multiple Input Multiple Output communication systems are able to provide an increased data rate, with consequently improved error performance as compared to systems without multiple antennas [1-4]. For antenna systems a particular area of interest is the practical utilisation of multi-path propagation [5, 7]. During the propagation of signals from the transmitter side, these transmitted signals reflected from intermediate objects which cause these signals to travel along separate paths with different time of arrival at the receiver end. These effects combined with digital beam-forming enhance the potential for greater system capability and bandwidth. In order to realize this potential it is necessary to understand how the use of spatial correlation based on polarization states impacts on the achievable volume of the radiating structures.

This paper presents the modeling and design concepts of 2×2 and 3×3 MIMO antenna systems for mobile handsets. The spatial, polarization technique has been used to improve the channel capacity of the system.

The channel capacity is estimated and discussed over Raleigh fading channel and compared to planar antenna array MIMO channel. In order to calculate the channel capacity several power spectrum distribution functions has been used [8-15].

Channel Capacity Model

A communication system which is comprised of N number of transmitter and receiver antennas, the channel capacity can be calculated by using the well-known formula [16],

$$C = \mathbb{E}\log_2\left|\left(\mathbb{I} + \frac{P_t}{n_t\sigma}\right)HH^{\dagger}\right| \quad (1)$$

Which is an expectation value incorporating, the variance of the noise power (σ), the mean of the total transmitted power (P_t), and the channel transfer matrix, H. The matrix size is $n_r \times n_r$, $\mathbb{I}$ is the identity, and '†' is the conjugate transpose operation. If the spatial matrices characterising the receiver (W_r) and transmitter (W_t) are also known, then $HH^{\dagger}$ may be obtained simply as follows:

$$HH^{\dagger} = W_r G_w W_t^{\dagger} \quad (2)$$

The characteristic channel properties are encoded in the system matrix G_w so for a channel with Rayleigh fading these matrix elements are drawn from a complex Gaussian distribution [17-19]. A further simplification can be introduced into the modelling, where the spatial transmitter matrix for maximum channel capacity is given as the identity, this is justifiable on physical grounds. For the maximum channel capacity the spatial matrix of the transmitter can be reduced to identity matrix due to the space availability at the transmitter side. Now equation (2) can be simplified to the following:

$$HH^{\dagger} = W_r G_w \quad (3)$$

The receiver spatial matrix W_r can be defined by the Following equation:

$$W_{r_{ij}} = \sqrt{\frac{\oiint d\Omega (E_{ai}\cdot E_i)(E_{ai}\cdot E_i)^*}{\sigma_1\sigma_2}} \quad (4)$$

Where

$$\sigma_j = \oiint d\Omega \left(E_{aj}\cdot E_j\right)^2 \quad (5)$$

The spatial integrals used in the above equations are understood to be parameterised as $\oiint = \int_{\phi_1}^{\phi_2}\int_{\theta_1}^{\theta_2}(\cdot)$ with measure $d\Omega = \sin\theta\, d\theta d\phi$. The E_{ai} are the electric fields of the radiating elemnts, whilst the E_i are the electric fields incidents on the receiver side.

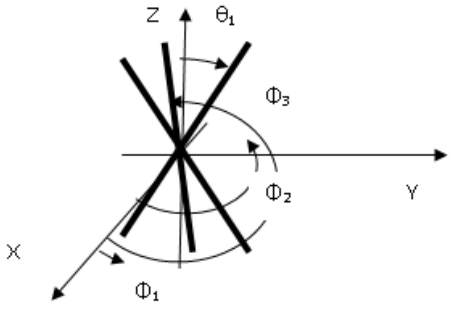

Fig.1. The basic antenna geometry for 3×3 system

The polarization geometry assumes a set of three collocated dipoles antennas present over the azimuthal axis whereas they are centred at the origin. Fig.1 and Fig.2 shows the geometric representation of the 3×3 and 2×2 proposed antenna systems. This analysis is restricted to a

maximum of three radiating elements; at this stage the mutual couplings are ignored. The elements are arranged according to the elevation angle which has been considered as polarization angle in this case. To reduce complexity, short dipoles are employed in which their radiating field can be easily computed.

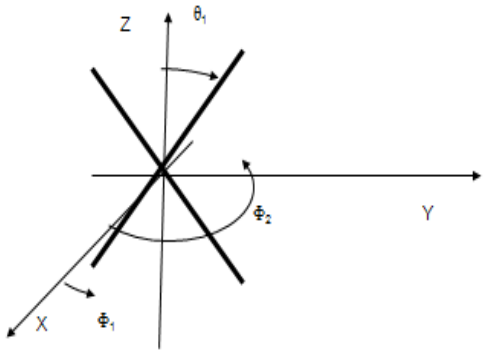

Fig.2. The basic antenna geometry for 2×2 system

However, for arbitrary dipole orientation in(θ_d, ϕ_d), the following unit vector, which defines the local axis of the dipole, can be expressed as follows:

(6). $\hat{d} = \sin\theta_d \cos\phi_d \hat{e}_x + \sin\theta_d \sin\phi_d \hat{e}_y + \cos\theta_d \hat{e}_z$

where $\{\hat{e}_i\}$ form an orthonormal right handed triad. The radiated dipole field can be given as follows:

(7) $E_a = E_\theta(\theta,\phi)\hat{e}_\theta + E_\phi(\theta,\phi)\hat{e}_\phi$

The components E_θ and E_ϕ are defined as the (spatially averaged) scalar products,

(8) $E_\theta(\theta,\phi) = \langle \hat{d} \cdot \hat{u}_\theta \rangle$

(9) $E_\phi(\theta,\phi) = \langle \hat{d} \cdot \hat{u}_\phi \rangle$

and

(10) $\hat{u}_\theta = \cos\theta\cos\phi\hat{e}_x + \cos\theta\sin\phi\,\hat{e}_y + \sin\theta\,\hat{e}_z$

(11) $\hat{u}_\phi = -\sin\phi\,\hat{e}_x + \cos\phi\,\hat{e}_y$

Power Spectrum Distribution Functions

For the calculation of the channel capacity of MIMO system, several power distribution functions have been used [20-23]. Gaussian, Laplacian and Secant squared, uniform distributions have been used over the azimuthal angle. In addition raised cosine and the nth order raised cosine distributions are considered along the zenith angle. These distributions are combined with one another to form the incident plane wave illuminating the receiver elements. The following analysis considers all possible combinations between these distributions in such a way as to predict the maximum degradations and/or improvements of the proposed MIMO system performance. In general, there are twelve combinations can be considered to compute the channel capacity of the MIMO system.

Gaussian distribution

The power spectrum over the azimuthal direction using a Gaussian distribution can be defined as follows:

(12) $P_\phi(\phi) = \sqrt{A}\exp\left\{-\frac{(\phi - m_\phi)^2}{2\sigma_\phi^2}\right\} \quad -\pi \le \phi \le \pi$

where A is the normalization factor, this can be given by:

(13) $A = 2\sigma_\phi^2\pi\left\{-\mathrm{erf}\left(\frac{-\pi+m_\phi}{\sqrt{2}\sigma_\phi}\right) + \mathrm{erf}\left(\frac{\pi+m_\phi}{\sqrt{2}\sigma_\phi}\right)\right\}^2$

m_ϕ and σ_ϕ are the mean and variance of the Gaussian function respectively. Several plots of this function for different values of m_ϕ and σ_ϕ are illustrated in Fig.3.

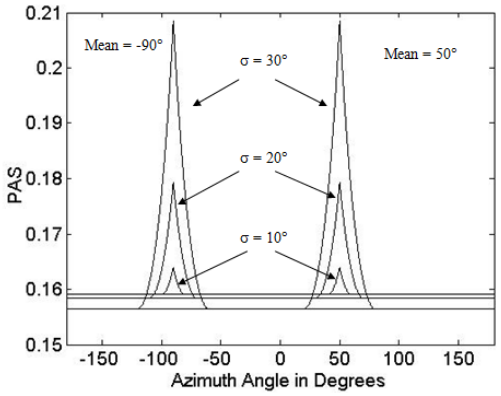

Fig.3.Gaussian distribution functions for different values of m_ϕ and σ_ϕ

Laplacian distribution

A well known practical channel capacity approximation uses the Laplace power distribution along azimuthal direction [24-26]. Laplacian distribution can be simply expressed as follows:

(14) $P_\phi(\phi) = \sqrt{A}\exp\left\{-\frac{|\phi - m_\phi|}{\sigma_\phi}\right\} \quad -\pi \le \phi \le \pi$

The behaviour of this distribution for different values of m_ϕ and σ_ϕ are illustrated in,Fig.4. Note that these distributions show narrower, and sharp variations, around the mean of the incident angle compared to that found in the Gaussian distributions.

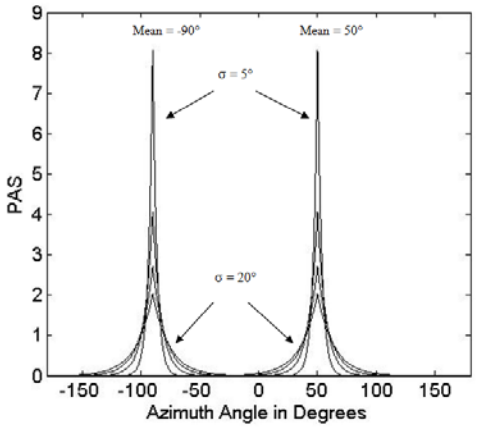

Fig.4. Laplacian distribution functions for different means and variances.

Secant square distribution

Raised (nth order) cosine distributions applied along an angular direction are also used in some applications when calculating the channel capacity. This distribution function can be expressed as follows,

(15) $P_\phi(\phi) = \frac{0.5}{(\pi-\phi_0)+\tan\phi_0}, -\pi \le \phi \le \pi$

$$\begin{cases} \sec(\phi_0 - |\pi - \phi_0|), |\phi - m_\phi| \le \phi_0 \\ 1, |\phi - m_\phi| > \phi_0 \end{cases}$$

where $2\phi_0$ is the width of the angle when the distribution is not constant, and m_ϕ is the mean angle in which the incident fields scattered on the antenna. Several distribution functions of this kind of PAS are shown in Fig.5.

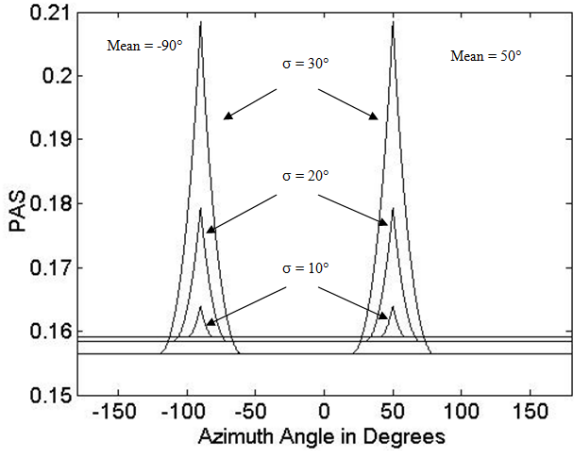

Fig 5. Secant square distribution functions for different m_ϕ and angular widths.

Raised cosine (nth order) distribution

Raised (nth order) cosine distributions applied along an angular direction are also sued in some applications when calculating the channel capacity. This distribution function can be expressed as follows,

$$(16)\ P_\theta(\theta) = A\left(1+\cos\left(\frac{2\pi(\theta-m_\theta)}{s}\right)\right)^n \quad \text{for } m_\theta - \frac{s}{2} \le \theta \le m_\theta + \frac{s}{2}$$

where m_θ is the mean angle, s is the total width angle and A is the normalization factor. The distribution functions for $n = 1, n = 2$ and $n = 4$ are shown in Fig 6 for different values of s and m_θ.

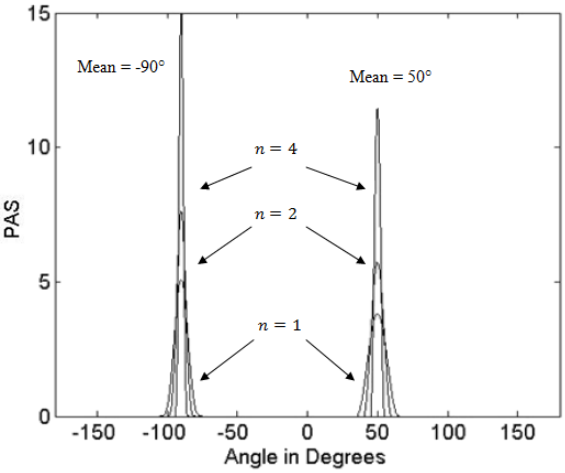

Fig 6. Raised Cosine distribution functions for different means and angle widths.

Channel Capacity Estimation and Results

With high signal to nose ratio the channel capacity can be given by:

$$(17)\qquad C = \sum_{i=1}^{n}\left(\mathbb{I} + \frac{P}{n_T\sigma}\lambda_i\right)$$

where λ_i (for $i = 1,2,3$) are the eignvalues of the matrix given in equation 17. However, the channel capacity is also computed for comparison using equation 1. The incident fields are assumed to have uniform distribution over the range $[0,2\pi]$ for azimuthal angle ϕ, and 30° over the elevation angle at the horizontal plane for an urban channel.

For suburban channels the variation over elevation angle is similar to the urban channel model. The azimuth is taken at 5° intervals from 5° to 20°, and the corresponding Laplacian spectra are computed and compared.

The E_θ and E_ϕ of the incident fields were assumed to be independent over the angular range$[\theta, \phi]$, and their variations are uniform for the channel models under consideration. It was also assumed that the phase variations are uniform over $[0,2\pi]$.

Channel capacities for an urban channel model are simulated for both the 2×2 and 3×3 MIMO systems, the results are shown in Fig 7 and Fig.8. The antennas for the 2×2 system are located at $\phi = 0°$ and $180°$, whereas for the 3×3 system $\phi = \{0°, 120°, 240°\}$. The data used to generate these figures employs a closed form solution for the elements of W_r. The capacity was evaluated over a Rayleigh fading model, the average was taken over 1000 complex samples. The transfer function was normalized at each point to provide a good prediction of the maximum variation of the spatial matrices for these MIMO antennas. It should be noted that the maximum capacities for the 2×2 and 3×3 cases occur at 55° and 63° respectively. These angles should be selected for the required orthogonalization of the spatial field distributions for the antenna geometry (in Fig.1).

The same sequence of results is presented for the suburban channel model in Fig.9 and Fig.10 for various values of σ_ϕ. Here the maximum capacity limits for the 2×2 MIMO case are reached for all the presented values of σ_ϕ; in the 3×3 case there is a slight, but detectable reduction, as σ_ϕ increases. The elevation angle is varied uniformly over 30 degrees at the horizontal plane, whereas azimuth angle varied as Laplacian spectrum of different values of σ_ϕ (5, 10, 15, 20 degrees for the geometry presented in Fig.1) in which the azimuth direction randomly selected between 0 and 2π.

Channel capacities for the 2×2 and 3×3 cases using the Secant square distribution along azimuth angle are shown in Fig.11 and Fig.12. The antennas for the 2×2 case are located at $\phi = 0°$ and$180°$, whereas for the 3×3 case $\phi = \{0°, 120°, 240°\}$. For the 2×2 and 3×3 systems the maximum channel capacities have been observed at 55° and 62° respectively. Fig.14 and Fig.15 show the channel capacities of 2×2 and 3×3 systems as described in figures 1 and 2 respectively. The channel capacity has been calculated by assuming the Raised cosine distributions along the zenith angle whereas Gaussian distribution has been used along the azimuth. In both cases the calculated channel capacity is seen to approach the maximum limit.

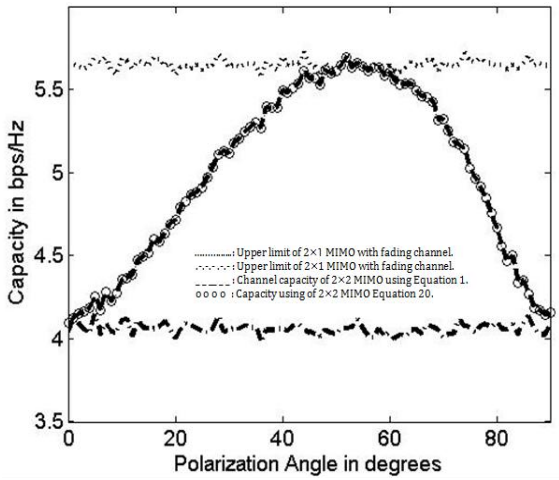

Fig 7. Computed Channel capacity with respect to polarization angle using Gaussian distribution for 2 × 2 MIMO system.

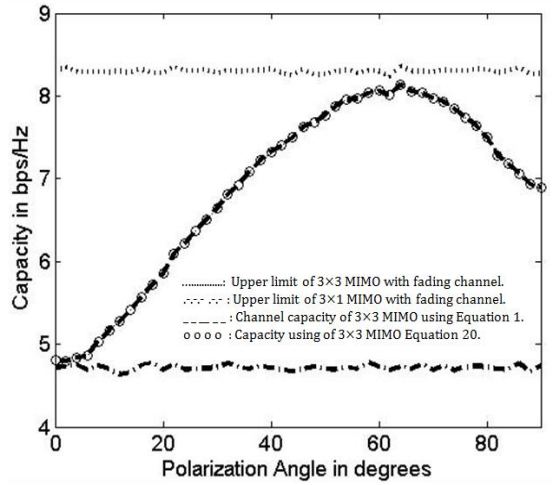

Fig 8. Computed Channel capacity with respect to polarization angle using Gaussian distribution for 3×3 MIMO system.

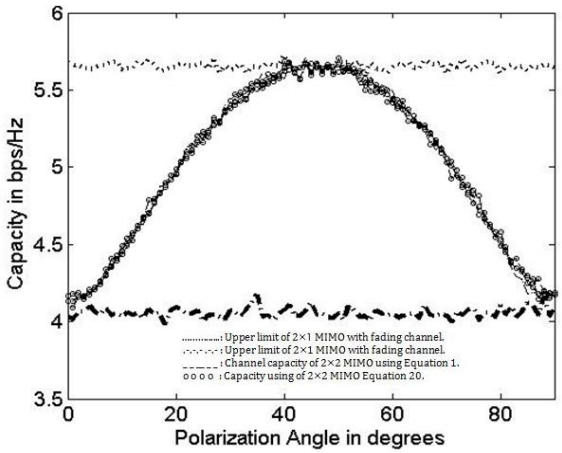

Fig 9. Computed Channel capacity with respect to polarization angle using Laplacian distribution, as antennas are rotated by 90° over azimuth, for 2 × 2 MIMO system.

It should be noted that the channel capacity results shown in Fig.13 and Fig.14 are approximately similar to the capacities calculated using Laplacian and Secant squared distributions. The maximum capacities for both 2×2 and 3×3 MIMO systems have been observed at the polarization angles of 64°.

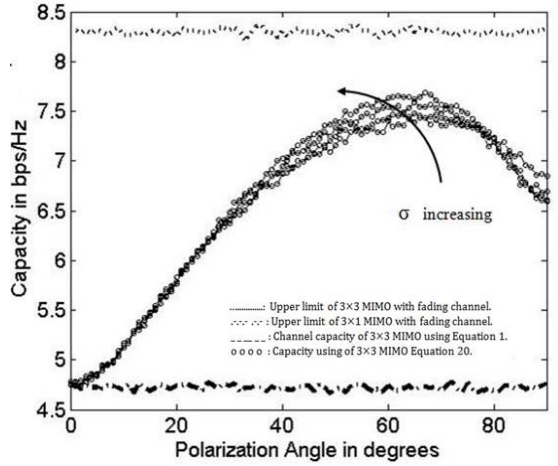

Fig 10. Computed Channel capacity with respect to polarization angle using Laplacian distribution, whereas antennas are located at 90°, 210°, and -30° at azimuth, for 3 × 3 MIMO system.

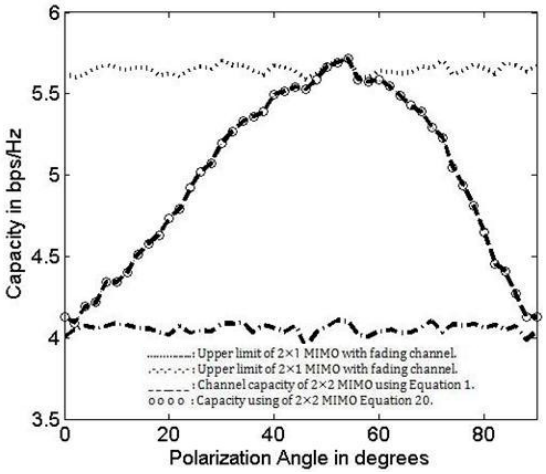

Fig 11. Computed Channel capacity with respect to polarization angle using secant square distribution for 2 × 2 MIMO system.

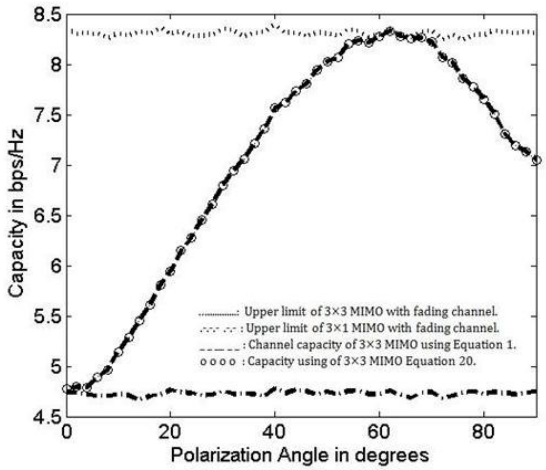

Fig 12.Computed Channel capacity with respect to polarization angle using secant square distribution for 3×3 MIMO system.

The channel capacities for different transmitted powers are shown in Fig.15, here the elevation angle varies uniformly over 180° from the centre (with zero crossings), but with the same azimuthal variations used for Fig.8 and Fig.10. The channel capacities can be seen to increase with increasing SNR (this is in fact approximately linear); with the maxima located at an elevation angle of 63°.

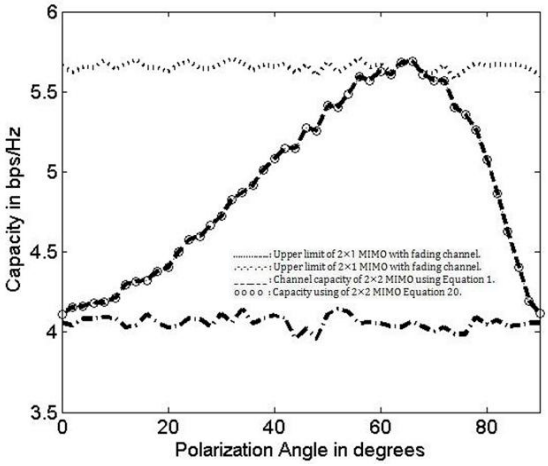

Fig.13.Computed Channel capacity with respect to polarization angle using raised cosine distribution for 2 × 2 MIMO system.

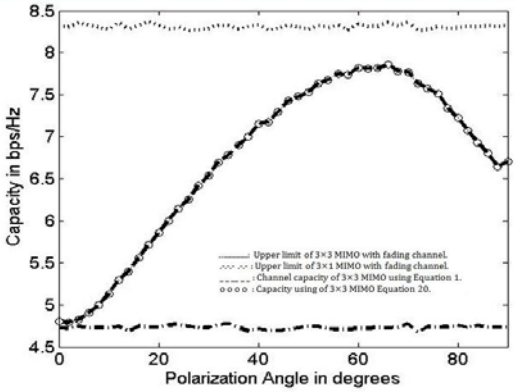

Fig.14. Computed Channel capacity with respect to polarization angle using raised cosine distribution for 3 × 3 MIMO system.

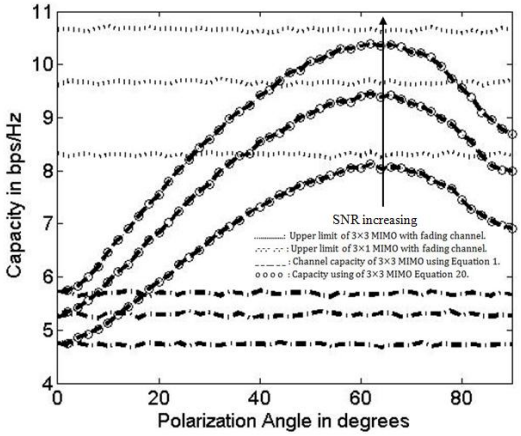

Fig.15.: Computed Channel capacity with respect to polarization angle for Signal to Noise ratio of 10dB, 15dB and 20dB for 3 × 3 MIMO system

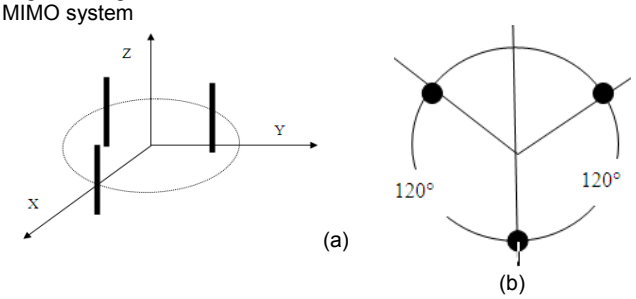

Fig.16. 3×3 MIMO ring antenna array system,(a) 3D geometry, (b) top view

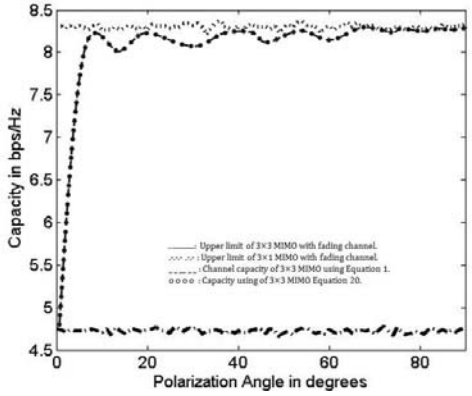

Fig.17.Computed Channel capacity with respect to radial distance in wavelength for 3 × 3 MIMO system shown in figure 16(a)(b) where the antennas are located at 0°, 120° and -120° azimuth

Fig.16 and Fig.17 shows a comparison, using the urban channel model, of the channel capacity for the MIMO antenna geometry vs. a simple planar ring array. The channel capacity of the planar ring is at a maximum when the ring radius is approximately $\lambda/4$ (i.e. the distance of separation between the elements is $\lambda/2$). These results clearly indicate the possible benefits for volume reduction using the MIMO antenna geometry proposed in Fig.1.

Conclusion

This research paper has thoroughly discussed the channel capacities for 2×2 and 3×3 Multiple Input Multiple Output systems with respect to spatial polarization technique. Furthermore verity of channel capacity results have been computed for MIMO systems presented in Figure 1 and Figure 2, these results have been simulated over Raleigh fading channel with different azimuthal spectra. The simulated results have been compared and verified using the dominant Eigen values related to the channel matrix. It has been concluded form the presented results that the maximum channel capacity can be reached for the tightly collocated multiple antennas by careful selection of the intrinsic orthogonalities of spatial field distribution. The estimated results for the proposed small volume geometry are comparable with planar array which has much larger antenna volume.

***Author**: Dr. Muhammad Usman, Assistant Professor of Electrical Engineering, Department of Electrical Engineering, College of Engineering, University of Hail, Kingdom of Saudi Arabia, Email: m.usman@uoh.edu.sa*

REFERENCES

[1] Da-Shan, G.J. Foschini, M.J. Gans and J.M. Kahn, "Fading Correlation and Its Effect on the Capacity of Multi-element Antenna Systems", IEEE Transactions on Communications,Vol.48, NO.3, March 2000.

[2] E. Biglirie, et al, "MIMO Wireless Communications", Chapters 1 – 3, John Wiley, NY, ISBN-978052187

[3] D. Tse and P. Viswanath, "Fundamentals of Wireless Communication", Chapters 7 – 10, Cambridge University Press, 2005.

[4] L. Dong, H. Choo, R.W. Heath, and H. Ling, "Simulation of MIMO Channel Capacity With Antenna Polarization Diversity", IEEE Transaction on Wireless Communication, Vol. 4, July 2005.

[5] Y. Takatori, F. Fitzek, K. Tsunekawa, R. Prasad, "Channel Capacity of TDD, OFDM MIMO for Multiple Access Points in a Wireless Single Frequency Network", MIMO MAP Springer 2005.

[6] G. J. Foschini and M. J. Gans, "On limits of wireless communication in a fading environment when using multiple antennas", Wireless Personal Commun., vol. 6, no. 3, pp. 311–335, Mar. 1998.

[7] G. J. Foschini and R. A. Valenzuela, "Initial estimation of communication efficiency of indoor wireless channel", Wireless Networks, vol. 3, pp. 141–154, 1997.

[8] J. W. Wallace and M. A. Jensen, "Modelling the indoor MIMO wireless channel", IEEE Trans. Antennas Propag., vol. 50, no. 5, pp. 591–599,May 2002.

[9] J.W. Wallace, M.A. Jensen, A.L. Swindlehurst, and B.D. Jeffs, "Experimental characterization of the MIMO wireless channel: Data acquisition and analysis", IEEE Trans. Wireless Commun., vol. 2, no. 2, pp. 335–343,Mar. 2003.

[10] D. Gesbert, H. Bölcskei, D.A. Gore, and A. Paulraj, "Outdoor MIMO wireless channels: Model and performance prediction", IEEE Trans. Commun., vol. 50, no. 12, pp. 1926–1934, Dec. 2002.

[11] L. Dong, H. Choo, R.W Heath and H. Ling, "Simulation of MIMO Channel Capacity with Antenna Polarization Diversity", IEEE Transactions on wireless communications, vol. 4, no. 4, July 2005, pp. 1869-1873.

[12] Usman, Muhammad. "Polarisation-Diverse MIMO System Performance for Mobile Phones Wlan Application." IJET-IJENS Vol:13 No:01 2013.
[13] C.E. Shannon, "A Mathematical Theory of Communication", Bell System Technical Journal, vol. 27, pp. 379-423, 623-656, July, October, 1948.
[14] Usman, Muhammad, Raed A. Abd-Alhameed, and Peter S. Excell. "Design considerations of MIMO antennas for mobile phones." PIERS (2008).
[15] Usman, M., R. A. Abd-Alhameed, Y. A. S. Dama, P. S. Excell, D. Zhou, B. Ibrahim, and E. A. Elkhazmi. "New compact dual polarised dipole antenna for MIMO communications." In Smart Antennas (WSA), 2010 International ITG Workshop on, pp. 326-330. IEEE, 2010.
[16] J.H. Winters, J. Salz, and R.D. Gitlin, "The impact of antenna diversity on the capacity of wireless communication systems", IEEE Trans. Commun., vol. 42, pp. 1740–1751, Feb. 1994.
[17] M.R. Andrews, P.P. Mitra, and R.de Carvalho, "Tripling the capacity of wireless communications using electromagnetic polarization", Nature, vol. 409, no. 6818, pp. 316–318, Jan. 2001.
[18] T. Svantesson, "On capacity and correlation of multi-antenna systems employing multiple polarizations", in IEEE Int. Antennas Propagation Symp. Digest, San Antonio, TX, Jun. 2002, pp. 202–205.
[19] D.D. Stancil, A. Berson, J.P. Van't Hof, R. Negi, S. Sheth, and P. Patel, "Doubling wireless channel capacity using co-polarised, co-located electric and magnetic dipoles", Electron. Lett., vol. 38, no. 14, pp. 746–747, Jul. 2002.
[20] H.D. Tuan, D. Pham, B. Vo, T.Q. Nguyen, "Entropy of General Gaussian Distributions and MIMO Channel Capacity Maximizing Precoder and Decoder", Acoustics, Speech and Signal Processing, 2007. ICASSP 2007. IEEE International Conference on Volume 3, Issue , 15-20 April 2007 Page(s):III-325 - III-328.
[21] G. Turin, F. Clapp, T. Johnston, S. Fine, and D. Lavry, "A statistical model of urban multipath propagation", IEEE Trans. Veh. Technol., vol.21, pp. 1–9, Feb. 1972.
[22] H. Suzuki, "A statistical model for urban radio propagation", IEEE Trans. Commun., vol. 25, pp. 673–680, July 1977.
[23] S.A. Zekavat and C.R. Nassar, "Power-azimuth-spectrum modelling for antenna array systems: a geometric-based approach", Antennas and Propagation, IEEE Transactions on Antennas and Propagation, Volume 51, Issue 12, Page(s):3292 – 3294, December 2003.
[24] K.I. Pedersen, P.E. Mogensen, and B.H. Fleury, "A Stochastic Model of the Temporal and Azimuthal Dispersion Seen at the Base Station in Outdoor Propagation Environments", IEEE Transactions on vehicular Technology, Vol .49,No.2, March 2000.
[25] P.C. Hsieh and F.C. Chen, " A new MIMO spatial correlation approximation of large angular spread", Antennas and Propagation Society International Symposium, 2007 IEEE Volume , Issue , 9-15 June 2007 Page(s):1909 – 1912.
[26] L.J. Dong, J. Ma, J. Zhou, and H. Kikuchi, " Performance of MIMO with UCA and Laplacian Angular Distribution Using Correlation Matrix", International Conference on Wireless Communications, Networking and Mobile Computing, 2007. WiCom 2007. 21-25 Sept. 2007 Page(s):53 – 56.